**The published version of the paper " L. Valentini, S. Bittolo Bon, M. Hernandez, M.A. Lopez-Manchado, N.M. Pugno (2018). Nitrile butadiene rubber composites reinforced with reduced graphene oxide and carbon nanotubes show superior mechanical, electrical and icephobic properties. Composites Science and Technology 166, 109-114." is available at: https://doi.org/10.1016/j.compscitech.2018.01.050.**

# Nitrile butadiene rubber composites reinforced with reduced graphene oxide and carbon nanotubes show superior mechanical, electrical and icephobic properties

L. Valentini[1*], S. Bittolo Bon[1], M. Hernández[2], M.A. Lopez-Manchado[2**], N. M. Pugno[3,4,5]

[1] *Civil and Environmental Engineering Department, University of Perugia, UdR INSTM, Strada di Pentima 4, 05100 Terni, Italy. E-mail: luca.valentini@unipg.it*

[2] *Instituto de Ciencia y Tecnología de Polímeros, ICTP-CSIC, Juan de la Cierva, 3 28006 Madrid, Spain. E-mail: lmanchado@ictp.csic.es*

[3]*Laboratory of Bio-Inspired and Graphene Nanomechanics, Department of Civil, Environmental and Mechanical Engineering, University of Trento, Trento - Italy*

[4]*School of Engineering and Materials Science, Queen Mary University of London, Mile End Road, London - United Kingdom.*

[5]*Ket Lab, Edoardo Amaldi Foundation, Italian Space Agency, via del Politecnico snc, I-00133 Roma, Italy*

**Abstract**

In this article, we examine the effects of two different nanostructured carbons when they are incorporated in a rubber matrix in terms of mechanical and electrical properties as well as the icephobic behaviour of the nanocomposites when swollen. Nitrile butadiene rubber composites reinforced with thermally reduced graphene oxide or multiwalled carbon nanotubes or both of them were prepared and characterized. At a particular hybrid filler loading, tensile and electrical tests showed a significant improvement of the composite. From the swelling studies, after the immersion, the nanocomposites experienced a reduction of the cross-link density that promotes weakening of ice adhesion, being this effect more evident for those samples prepared with hybrid fillers. In view of the composite formulations, that utilize commercially available elastomers and fillers, these findings would be applicable to the automotive and aviation sectors, where the demand for multifunctional rubbers is increasing.

Keywords: graphene; carbon nanotubes; mechanical properties; icephobic, rubber nanocomposites.

## Introduction

Nanocarbons such as carbon nanotubes (CNTs) and graphene nanoplatelets exhibit superior -at least ideal- mechanical and electrical properties compared to other nanofillers, making them ideal candidates as fillers for polymer nanocomposites used in advanced applications [1-5]. Thus, an important use of such nanomaterials is in reinforcing polymer matrices taking advantage of the ultra-high stiffness and electrical conductivity exhibited by them. The nanotube dispersion and deformation mechanisms in polymer composites was addressed by Qian et al. [6] who studied a model composite system in which carbon nanotubes were dispersed in a polystyrene matrix, while Xie et al. [7] predicted theoretically that graphene is more effective for electrical conductivity than CNTs because of its large specific surface area even if, in this regard, there are contradictory studies stating that graphene is less effective than CNTs in forming conductive percolated networks [8].

Some of the recent researches have combined CNTs with other fillers. Prasad et al. [9] reported the extraordinary synergy effect in the mechanical properties of polymer matrix composites when reinforced with two different nanocarbons. It was also found that graphene and CNTs enhanced the mechanical properties of silicone rubber [10]; Bokobza et al. [11] reported the stress-strain improvement in styrene–butadiene rubber when a blend of carbon black and CNTs were used while Valentini et al. [12] reported the synergistic effect of graphene nanoplatelets and carbon black in EPDM nanocomposites. Other findings showed how hybrid carbon nanofillers had synergistic effects in electrical conductivity, thermal conductivity and mechanical properties [13-15].

Graphitic compounds (CNTs, graphene), compared to other conventional types of fillers, exhibit a significant ability to enhance mechanical and other functional properties of a rubber-like matrix, especially in the case of fine dispersion in the host medium, which acts in favor of the enhanced interfacial interaction. Nitrile butadiene rubber (NBR) is commonly considered the workhorse of the industrial and automotive rubber products because of its good mechanical properties, its resistance to lubricants and greases and its relatively low cost. Efforts also have to be done to find

more suitable filler for NBR in order to achieve high performance products with higher tensile strength and electrical conductivity, being the mechanisms behind the synergetic effects of hybrid fillers in this matrix not completely understood. Moreover, there is a need to develop high performance elastomeric materials in extreme environments; for example, there is now and will continue to be, a need to develop high performance elastomeric sealing materials for oil and gas applications for primary use in the exploration and operational drilling applications, in ever unexplored locations of the northern hemisphere; this makes the icing issue of great attention. In such extreme conditions, icing problems will become more hazardous, limiting activities at oil and gas extraction unless reliable solutions are found.

In the frame of the presented work, NBR composites were prepared using thermally reduced graphene oxide (TRGO) or CNTs or both of them (hybrid, i.e. TRGO+CNTs) as fillers. We were also interested in investigating the physical properties and swelling of neat NBR and respective TRGO/CNT composites and in understanding their surface adhesion properties with specific attention to ice.

**Experimental details**

NBR under the trade name Krynac 2850F (acrylonitrile content: 27.5 wt.%, Mooney viscosity $M_L$ (1+4) 100 ºC 48 and a density of 0.97 g/cm$^3$) was used as rubber matrix. TRGO was synthetized in our laboratories following the procedures described elsewhere [16]. CNTs were kindly supplied by Nanocyl S.A. under the trade name Nanocyl NC7000.

Rubber compounds were prepared in an open two-roll mill at room temperature. The rotors operated at a speed ratio of 1:1.4. The vulcanization ingredients were sequentially added to the rubber before to the incorporation of the filler and sulphur. The recipes of the compounds are described in Table 1. Vulcanizing conditions (temperature and time) were previously determined by

a Monsanto Moving Die Rheometer MDR 2000E. Rubber compounds were then vulcanized at 160 ºC in a thermofluid heated press. The vulcanization time of the samples corresponds to the optimum cure time $t_{90}$ derived from the curing curves of the MDR 2000E.

The filler volume fraction was calculated from the well-known relationship: $f=(W_f/\rho_f)/(W_f/\rho_f + W_m/\rho_m)$, where $W_f$ is the weight fraction of the filler and $W_m$ is the weight fraction of the matrix, while $\rho_f$ and $\rho_m$ are the densities of the filler (i.e. 0.066 g/cm$^3$ [17] for CNTs and 2.2 g/cm$^3$ for TRGO [18]) and the matrix, respectively. For the case of the hybrid filler, the equation was extended in order to take into account the presence of both fillers in the matrix volume.

*Table 1. Recipes of the rubber compounds (indicated in phr: parts per hundred of rubber)*

| sample | NBR | ZnO | Stearic acid | MBT | S | TRGO | CNT |
|---|---|---|---|---|---|---|---|
| NBR-0 | 100 | 5 | 1.5 | 1.5 | 1.5 | 0.0 | 0.0 |
| NBR-1 | 100 | 5 | 1.5 | 1.5 | 1.5 | 1.0 | 0.0 |
| NBR-2 | 100 | 5 | 1.5 | 1.5 | 1.5 | 3.0 | 0.0 |
| NBR-3 | 100 | 5 | 1.5 | 1.5 | 1.5 | 5.0 | 0.0 |
| NBR-4 | 100 | 5 | 1.5 | 1.5 | 1.5 | 0.0 | 1.0 |
| NBR-5 | 100 | 5 | 1.5 | 1.5 | 1.5 | 0.0 | 3.0 |
| NBR-6 | 100 | 5 | 1.5 | 1.5 | 1.5 | 0.0 | 5.0 |
| NBR-7 | 100 | 5 | 1.5 | 1.5 | 1.5 | 0.5 | 0.5 |
| NBR-8 | 100 | 5 | 1.5 | 1.5 | 1.5 | 1.5 | 1.5 |
| NBR-9 | 100 | 5 | 1.5 | 1.5 | 1.5 | 2.5 | 2.5 |
| NBR-10 | 100 | 5 | 1.5 | 1.5 | 1.5 | 1.0 | 5.0 |
| NBR-11 | 100 | 5 | 1.5 | 1.5 | 1.5 | 5.0 | 1.0 |

Tensile stress-strain properties were measured according to ISO 37-1977 specifications, on an Instron dynamometer (Model 4301), at 25 ºC at a crosshead speed of 500 mm min$^{-1}$. At least five specimens of each sample type were tested. The samples were then cut into strips of ~ 100 mm × 20 mm × 0.13 mm, the electrical resistance was measured using a computer controlled Keithley 4200 source. The electrical resistance measurements were performed by biasing the sample between two strips of silver paint located at a distance of 25 mm.

Trans-1,2-dichloroethylene was used as fluid for immersion. The specimens have been immersed in the fluid for 70 hours at the temperatures of 25°C. Test procedure was in accordance with ASTM D 471; at the end of the required immersion period, the specimens were cooled down to room temperature for 30 to 60 min, then dipped quickly in acetone at room temperature, and blot lightly with filter paper. The swelling studies were performed on a known volume and weight of vulcanized rubber in the form of a rectangular sample that was taken for swelling measurements in immersion liquids. After attaining equilibrium swelling (70 hours), its weight was recorded and the volume variation was estimated according to ASTM D 471. The "ice adhesion strength" was measured using a custom setup, where a force transducer was fixed to a slipping table, as the maximal force needed to delaminate the ice agglomerate divided by its contact area with the NBR (thus it is just an indication of the mean value of the shear stress under the testing conditions, Table 2). Prisms with the dimension of 10 mm×10 mm×6 mm were positioned on the sample surface and then filled with water. They were then frozen 12 hours at -20°C. The shear force was applied at a distance of 1 mm about the prism-elastomer interface. Testing was done at −10°C.

**Results and discussion**

The mechanical properties of the samples filled with CNTs, TRGO and hybrid fillers were evaluated by tensile testing (Figs. 1a-d) and the results are summarized in Tables 2 and 3. The addition of the TRGO and CNTs as a sole reinforcement as well as the addition of both of them causes a sensible increase of the stress at several elongations, tensile strength and fracture strength of the NBR composites. The reinforcing effect of both nanoparticles is more marked as the elongation is increased, reaching improvements of the maximum strength of 150 and 315% for nanocomposites containing 5 phr of TRGO and CNTs, respectively. In addition, this improvement does not imply a deterioration of the elastic properties of the material: all nanocomposites exhibit a higher elongation at break in relation to pristine rubber. Moreover, it was found that the two fillers

usually do not act in synergy here with respect to strength, see Table 2, where the equivalent strength of the filler is estimated from a classical direct rule of mixture.

Note that the addition of 5 phr TRGO alone to NBR leads to an enhancement in tensile strength of NBR by *p* as shown in Fig. 1a. Likewise, *q* represents the enhancement in tensile strength of NBR due to the addition of 1 phr CNTs alone in Fig. 1b. The synergistic effect or percent synergy attained by adding both 5 phr TRGO and 1 phr CNTs to NBR can also be computed as suggested by Prasad et al. [9] by the following relation: $[M_h-(p+q)]*100/(p+q)$, where $M_h$ is the measured value for the composite, Fig. 1d, for strength, elongation at break and toughness. The positive value of the synergy also for the strength for the hybrid 5/1 is due to the different definition with respect to the previous approach based on the filler equivalent strength, as reported in Table 2.

*Table 2. Filler volume fraction (f) and filler equivalent strengths of the prepared composites.*

| TRGO/CNTs | *f* | Filler equivalent strength (MPa) |
|---|---|---|
| 0/0 | 0 | - |
| 1/0 | 0.004 | 390.22 |
| 3/0 | 0.013 | 193.04 |
| 5/0 | 0.023 | 130.71 |
| 0/1 | 0.130 | 15.88 |
| 0/3 | 0.310 | 14.28 |
| 0/5 | 0.436 | 16.01 |
| 0.5/0.5 | 0.071 | 19.84 |
| 1.5/1.5 | 0.189 | 19.25 |
| 2.5/2.5 | 0.284 | 18.39 |
| 1/5 | 0.440 | 15.00 |
| 5/1 | 0.152 | 30.57 |

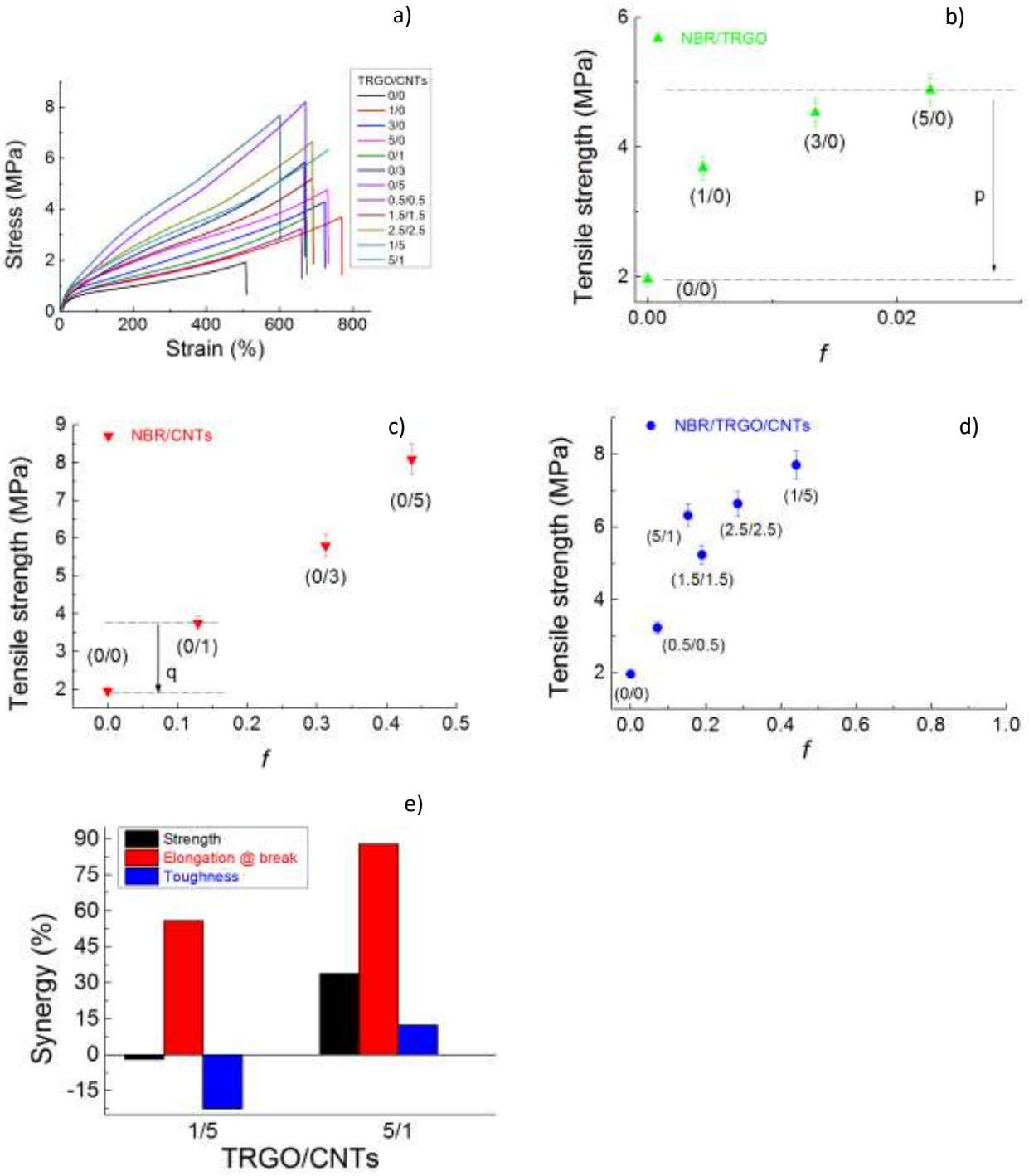


Figure 1. (a) Stress-strain curves and (b-d) maximum strength of the NBR composites filled with different types of nanostructured carbon fillers. The filler composition (TRGO/CNTs) in phr (parts per hundred rubber) is also indicated. (e) Percentage synergy in strength, elongation at break and toughness for two different binary composites.

*Table 3. Mechanical properties of NBR compounds.*

| **Sample** | Stress 50% elongation MPa | Stress 100% elongation MPa | Stress 300% elongation MPa | Stress 500% elongation MPa | Max Strength MPa | Elongation at break % | Toughness MPa |
|---|---|---|---|---|---|---|---|
| NBR-0 | 0.62±0.02 | 0.78±0.02 | 1.23±0.03 | 1.89±0.04 | 1.96±0.11 | 508±43 | 4.97±0.10 |
| NBR-1 | 0.73±0.01 | 0.93±0.01 | 1.51±0.01 | 2.26±0.02 | 3.68±0.39 | 756±66 | 13.91±0.13 |
| NBR-2 | 0.91±0.02 | 1.16±0.03 | 2.08±0.05 | 3.03±0.07 | 4.53±0.42 | 739±43 | 16.73±0.10 |
| NBR-3 | 1.05±0.02 | 1.35±0.03 | 2.44±0.07 | 3.36±0.11 | 4.88±0.57 | 735±61 | 17.93±0.14 |
| NBR-4 | 0.73±0.01 | 0.99±0.01 | 1.75±0.02 | 2.63±0.04 | 3.76±0.26 | 671±38 | 12.61±0.09 |
| NBR-5 | 0.94±0.02 | 1.41±0.05 | 2.90±0.10 | 4.30±0.21 | 5.81±0.32 | 647±39 | 18.79±0.08 |
| NBR-6 | 1.08±0.01 | 1.69±0.01 | 3.89±0.02 | 5.93±0.04 | 8.09±0.26 | 670±41 | 26.37±0.07 |
| NBR-7 | 0.71±0.03 | 0.93±0.06 | 1.54±0.11 | 2.30±0.16 | 3.23±0.47 | 652±29 | 10.82±0.15 |
| NBR-8 | 0.94±0.02 | 1.33±0.04 | 2.50±0.07 | 3.63±0.10 | 5.24±0.63 | 693±22 | 18.15±0.12 |
| NBR-9 | 1.17±0.04 | 1.76±0.09 | 3.26±0.10 | 5.06±0.22 | 6.64±0.33 | 672±33 | 22.31±0.07 |
| NBR-10 | 1.32±0.06 | 2.10±0.12 | 4.43±0.16 | 6.53±0.18 | 7.70±0.18 | 611±24 | 23.52±0.05 |
| NBR-11 | 1.15±0.02 | 1.59±0.03 | 3.05±0.05 | 4.24±0.07 | 6.32±0.60 | 733±61 | 23.16±0.13 |

The ratio of the volume fraction of the swollen rubber ($V_0$) and swollen filled rubber ($V_f$), respectively, has a direct relationship with the crosslink of the filler with the rubber matrix and thus estimates the interaction of the filler and matrix. Fig. 2 shows the plot of $V_0/V_f$ against $f/(1-f)$ according to Kraus equation [19,20]:

$$V_0/V_f = 1\text{-m } f/(1-f) \qquad \text{Eq. 1}$$

where $f$ is the volume fraction of the filler in the vulcanized rubber, $m$ represents the polymer-filler interaction parameter obtained from the opposite (in sign) of the slope of the plot of $V_0/V_f$ against $f/(1-f)$: the higher the $-m$ value, the better polymer–filler interaction [21]. This can also be seen in Fig. 2, where the Kraus plot of single phase and hybrid composites are reported. According to these results, with hybrid fillers the slope becomes steeper than that of CNT based composite, indicating higher rubber–filler interaction, confirming some of the trends reported in Table 2, specifically that the 5/0 and 5/1 solutions are the best among those treated here.

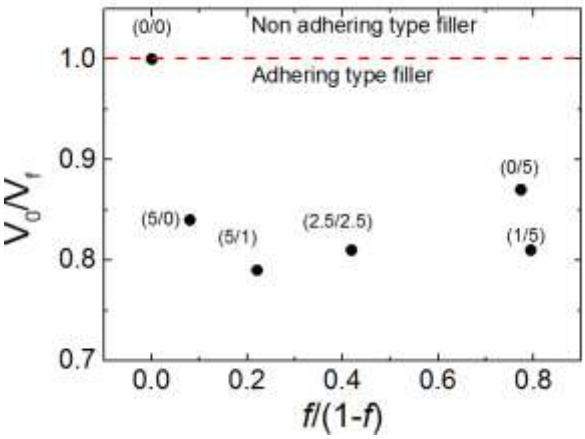


Figure 2. Kraus' plot for composites with various fillers.

Fig. 3 shows the electrical conductivity dependence on filler loading for the prepared nanocomposites. With a graphene loading to 0.02 volume fraction, the electrical conductivity was about $4.3 \times 10^{-10}$ S/m (Fig. 3a). At the CNT volume fraction of 0.31, the conductivity was $6 \times 10^{-6}$ S/m (Fig. 3b), which already exceeds the common value for surpassing the antistatic criterion, namely $10^{-6}$ S/m. Interestingly, for the hybrid composites we observed (Fig. 3c) a rise of the conductivity to $1 \times 10^{-4}$ S/m with a filler content of 0.43 volume fraction, which corresponds to the hybrid formulation 1/5. The aspect ratio of the fillers is the most important factor affecting the percolation threshold, that would decrease with increasing aspect ratio. The effect of aspect ratio can be explained by the excluded volume theory. The excluded volume is defined as the volume around an object into which the center of another similar object is not allowed to enter if interpenetration of the two objects has to be avoided. Thus, the higher aspect ratio induces the larger excluded volume, and thus lowers the percolation threshold. The conductive percolation threshold ($\varphi_p$) can be related to the aspect ratio ($A_f$) by the following equation [22-25]:

$$A_f = 3\varphi_{sphere}/2\varphi_p \qquad \text{Eq. 2}$$

where $\varphi_{sphere} = 0.30$ is a factor assuming the interaction of layered structures with an excluded volume assimilated to 3D percolating spheres [26]. Substituting in Eq. 2 the percolation volume fraction reported in Fig. 3 we estimated an increase of the aspect ratio from 1.4 to 19 passing from

the NBR/CNTs to NBR/TRGO composite, respectively. This means that the excluded volume of a network of TRGO is higher than that of a network of CNTs, suggesting a more densely packed network for CNTs in the hybrid composition.

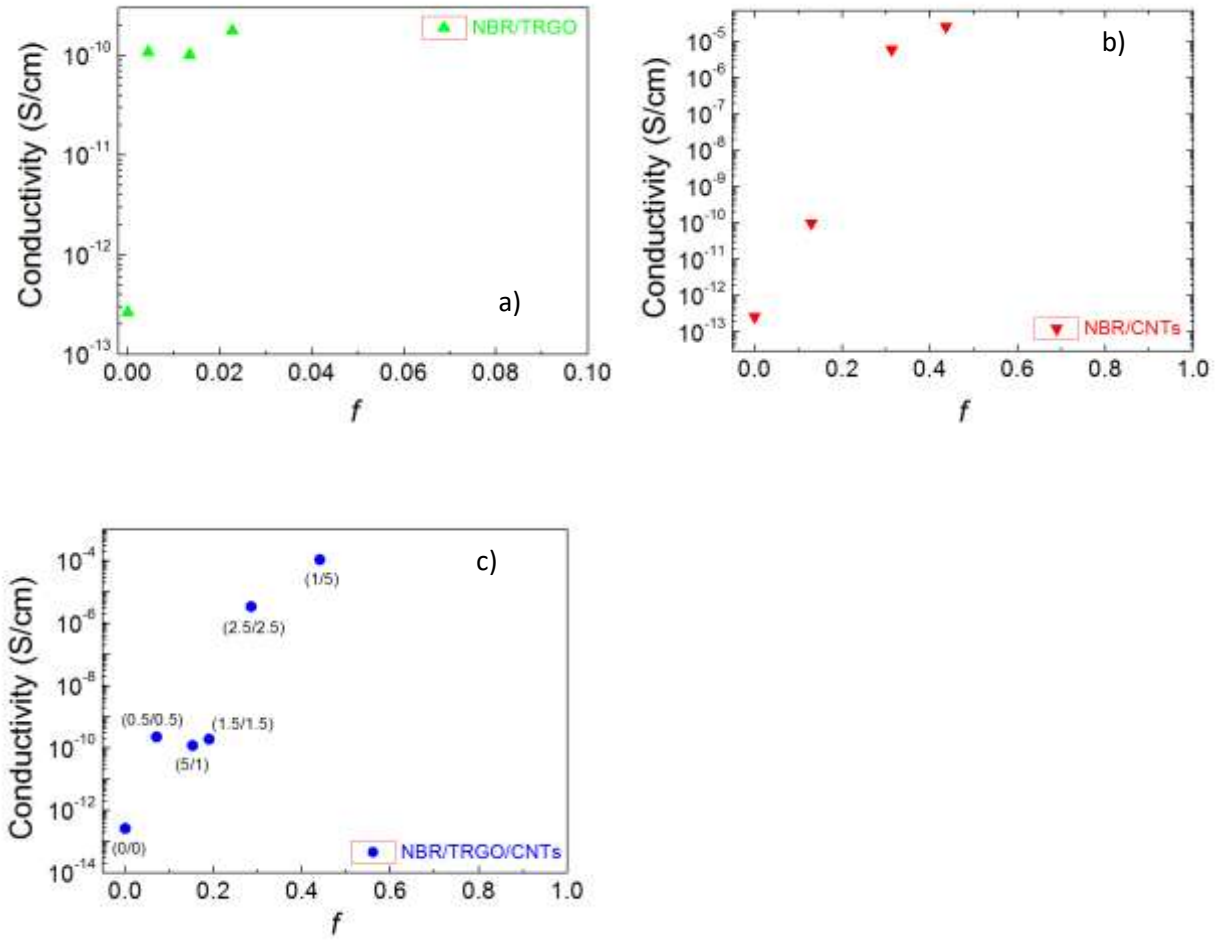


Figure 3. (a-c) Electrical conductivity of the nanocomposites as a function of filler volume fraction.

In the case of vulcanized rubbers, the polymer consists of a network structure of cross-linked chains that limit the amount of liquid that can be absorbed. Thus the greater the number of cross bonds in the elastomer the less it will swell. The swelling is thus an equilibrium state obtained when the dimensions of the elastomer increase until the concentration of the liquid is uniform throughout the component [27]. This relationship is quantitatively expressed by the Flory-Rehner equation [28, 29]:

$$\rho_{CL}=[\ln(1-V_r)+V_r+\chi V_r^2]/V[V_r^{1/3}-0.5V_r] \quad \text{Eq. 3}$$

where $V_r$ is the volume fraction of polymer in a swollen state, $\chi$ is the Flory-Huggins interaction parameter between the polymer and the solvent and V is the molar volume of the solvent.

According to the Flory and Rehner theory [29], originally derived for natural rubber vulcanized with carbon black, assuming that rigid fillers within the elastic network would not swell in the presence of a solvent, we calculate the volume fraction of the liquid within the swollen elastomers from the well-known relationship:

$$\Phi_{LIQUID}=(W_{LIQUID}/\rho_{LIQUID})/(W_{LIQUID}/\rho_{LIQUID} + f + W_m/\rho_m), \quad \text{Eq. 4}$$

where $W_{LIQUID}$ is the weight fraction of the liquid calculated from the relative difference of the weights of the sample in its dry and swollen state, $f$ is the volume fraction of the filler and $W_m$ is the weight fraction of the matrix, while $\rho_{LIQUID}$ and $\rho_m$ are the densities of the liquid and polymer matrix, respectively. For large values of swelling (i.e. small values of $\nu$=1/S DEFINE S), the molecular weight per chain ($M_c$) can be expressed as [29]

$$M_c \sim 2\rho V/(\nu)^{5/3} \quad \text{Eq. 5}$$

where $\rho$ is the polymer density. Eq. 5 states that the molecular weight between cross-links will increase with increasing the swelling; applying this equation to the high swollen state of TRGO/CNT composites in trans-1,2-dichloroethylene, the values of $M_c$ were calculated and reported in Tab. 4. In Fig. 5a, we show the relationship between the swelling and the cross-link density; the data indicate how a certain amount of liquid reduces the cross-link density of the prepared composites.

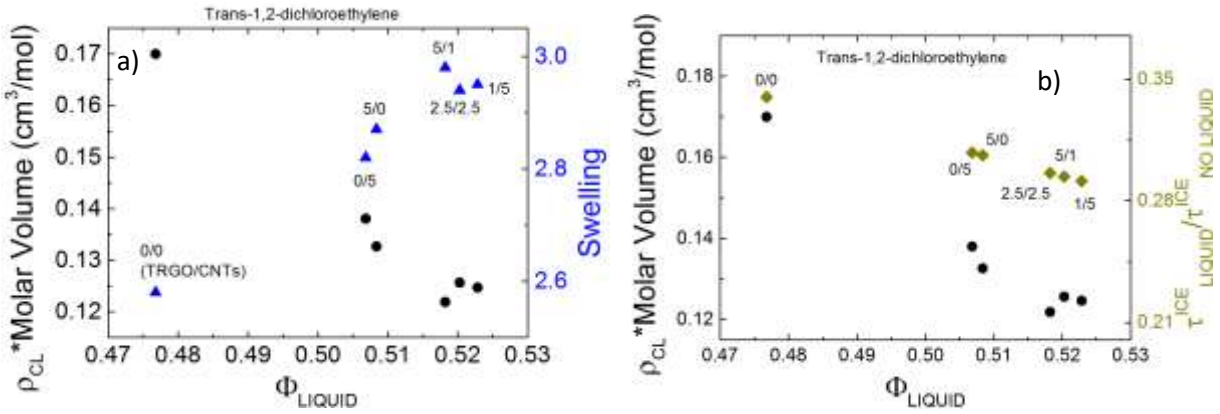


Figure 4. (a) Swell ratio and cross-link density reduction of liquid-filled TRGO/CNTs nanocomposites. (b) Measured ice adhesion strength $\tau^{ice}$ for NBR nanocomposites obtained with different TRGO/CNTs combinations as a function of the liquid volume fraction.

*Table 4. Nanocomposites reported in Table 1 and resulting swelling ratios, liquid volume fraction ($\Phi_{LIQUID}$) before and after liquid immersion and molecular weight between cross-links. The superscript (*) indicates the properties after the immersion in trans-1,2-dichloroethylene.*

| TRGO/CNTs | Swelling | $\Phi_{LIQUID}$ | $M_c$ (g/mol) |
|---|---|---|---|
| 0/0 | - | - | - |
| 0/0* | 2.58 | 0.477 | 781 |
| 5/0 | - | - | - |
| 5/0* | 2.82 | 0.506 | 889 |
| 0/5 | - | - | - |
| 0/5* | 2.87 | 0.508 | 924 |
| 2.5/2.5 | - | - | - |
| 2.5/2.5* | 2.94 | 0.520 | 953 |
| 1/5 | - | - | - |

| | | | |
|---|---|---|---|
| 1/5* | 2.95 | 0.522 | 967 |
| 5/1 | - | - | - |
| 5/1* | 2.98 | 0.518 | 983 |

Ice adhesion mechanisms at polymer interface can be at least roughly understood if we idealize the elastomer as a 'connector molecules' [30], that is, polymer chains are bound to the interface by physisorbtion, and interact with the bulk polymer so that they act to transmit stress across the interface. Assuming that during the ice detachment a chain with *n* monomers of size *a* is partially extracted, we could associate this with the pull-out energy proposed by Gennes et al. [31], where the free energy is a combination of the surface energy required to extract the chain and the elastic energy associated with the stretching of the extracted portion of the chain. Assuming the adhesion strength proportional to the surface tension that rescales with the inverse of the *n*a* (i. e. $M_c$) [31], we find a good matching between the cross-link density and the results reported in Fig. 5b where we present the ice adhesion data for the prepared nanocomposites after liquid immersion, where $\tau^{ice}_{liquid}$ is the adhesion strength of liquid filled sample while $\tau^{ice}_{no\ liquid}$ is the adhesion strength of the un-filled sample. In particular we observed, the reduction in ice adhesion strength ratio between the swollen and un-swollen TRGO/CNTs/NBR nanocomposite with the decrease (increase) of the cross-link density (molecular weight per chain).

## Conclusions

The mechanical strength and electrical conductivity of NBR composites containing independent or hybrid fillers of TRGO and CNTs were investigated. The results suggested that there are optimal concentrations of nanofillers for achieving the maximum strength and electrical conductivity of the composites. Materials with the highest reduction of the cross-link density show a lowest interfacial

interaction. A hybrid TRGO/CNTs system decreases the ice adhesion strength to the rubber material. We rationalized such results calculating the molecular weight between cross-links, and the adhesion strength according to the adhesion mechanisms at soft polymer interfaces, that can be modelled in terms of relays of dissipation mechanisms acting at different length scales, from molecular to macroscopic. We foresee such rubber nanocomposites having applications in several industrial areas where rubber based components need to operate in extreme environments.

**Acknowledgements**

N.M.P. is supported by the European Commission H2020 under the Graphene Flagship Core 1 No. 696656 (WP14 "Polymer composites") and FET Proactive "Neurofibres" grant No. 732344.

References

[1] Kostopoulos V, Vavouliotis A, Karapappas P, Tsotra P, Paipetis A. Damage monitoring of carbon fiber reinforced laminates using resistance measurements. Improving sensitivity using carbon nanotube doped epoxy matrix system. J Intell Mater Syst Struct 2009;20:1025 – 34.

[2] Badamshina E, Estrin Y, Gafurova M. Nanocomposites based on polyurethanes and carbon nanoparticles: preparation, properties and application. J Mater Chem A 2013;1: 6509-6529.

[3] Potts JR, Dreyer DR, Bielawski CW, Ruoff RS. Graphene-based polymer nanocomposites Polymer 2011;52:5 – 25.

[4] Cai D, Song M. Recent advance in functionalized graphene/polymer nanocomposites. J Mater Chem 2010;20: 7906-7915.

[5] Verdejo R, Bernal MM, Laura J. Romasanta LJ, Lopez-Manchado MA. Graphene filled polymer nanocomposites. J Mater Chem 2011:21:3301-3310.

[6] Qian D, Dickey EC, Andrews R, Rantell T. Load transfer and deformation mechanisms in carbon nanotube-polystyrene composites. Appl Phys Lett 2000;76:2868-2870.

[7] Xie S, Liu Y, Li JY. Comparison of the effective conductivity between composites reinforced by graphene nanosheets and carbon nanotubes. Appl Phys Lett 2008;92:243121-243123.

[8] Du JH, Zhao L, Zeng Y, Zhang LL, Li F, Liu PF. Comparison of electrical properties between multi-walled carbon nanotube and graphene nanosheet/high density polyethylene composites with a segregated network structure. Carbon 2011;49:1094 – 1100.

[9] Prasad KE, Das B, Maitra U, Ramamurty U, Rao CNR. Extraordinary synergy in the mechanical properties of polymer matrix composites reinforced with 2 nanocarbons. Proc Natl Acad Sci USA 2009;1060:13186–13189.

[10] Hu H, Zhao L, Liu J, Liu Y, Cheng J, Luo J, et al. Enhanced dispersion of carbon nanotube in silicone rubber assisted by graphene. Polymer 2012;53:3378-3385.

[11] Bokobza L, Rahmani M, Belin C, Bruneel JL, El Bounia, NE. Blends of carbon blacks and multiwall carbon nanotubes as reinforcing fillers for hydrocarbon rubbers. J Polym Sci 2008;46:1939-1951.

[12] Valentini L, Bittolo Bon S, Lopez-Manchado MA, Verdejo R, Pappalardo L, Bolognini A, et al. Synergistic effect of graphene nanoplatelets and carbon black in multifunctional EPDM nanocomposites. Comp Sci and Technol 2016;128:123-130.

[13] Chatterjee S, Nafezarefi F, Tai NH, Schlagenhauf L, Nüesch FA, Chu BTT. Size and synergy effects of nanofiller hybrids including graphene nanoplatelets and carbon nanotubes in mechanical properties of epoxy composites. Carbon 2012;50: 5380 – 5386.

[14] Maiti S, Shrivastava NK, Suin S, Khatua BB. Polystyrene/MWCNT/graphite nanoplatelet nanocomposites: efficient electromagnetic interference shielding material through graphite nanoplate-MWCNT-graphite nanoplate networking. ACS Appl Mater Interfaces 2013;5: 4712-4724.

[15] Yang SY, Lin WN, Huang YL, Tien HW, Wang JY, Ma CC M, et al. Synergetic effects of graphene platelets and carbon nanotubes on the mechanical and thermal properties of epoxy composites. Carbon 2011;49: 793 – 803.

[16] Aguilar-Bolados H, Lopez-Manchado MA, Brasero J, Aviles F, Yazdani-Pedram, M. Effect of the morphology of thermally reduced graphite oxide on the mechanical and electrical properties of natural rubber nanocomposites. Composites Part B 2016:87:350-356.

[17] Krause B, Mende M, Pötschke P, Petzold G. Dispersability and particle size distribution of CNTs in an aqueous surfactant dispersion as a function of ultrasonic treatment time. Carbon 2010;48:2746-2754.

[18] Gao C, Zhang S, Wang F, Wen B, Han C, Ding Y, et al. Graphene networks with low percolation threshold in abs nanocomposites: selective localization and electrical and rheological properties. ACS Appl Mater Interfaces 2014;6:12252–12260.

[19] Guth E. Theory of filler reinforcement. J Appl Phys 1945;16:20–25.

[20] Kraus G. Swelling of filler-reinforced vulcanizates. J Appl Polym Sci 1963;7:861-871.

[21] Paul KT, Pabi SK, Chakraborty KK, Nanodi GB. Nanostructured fly ash–styrene butadiene rubber hybrid nanocomposites. Polym Comp 2009;30:1647-1656.

[22] White SI, Mutiso RM, Vora PM, Jahnke D, Hsu S, Kikkawa JM, et al. Electrical percolation behavior in silver nanowire–polystyrene composites: simulation and experiment. Advanced Functional Materials 2010;20:2709-2716.

[23] Kim H, Macosko CW. Processing-property relationships of polycarbonate/graphene composites. Polymer 2009;50:3797-3809.

[24] Philipse AP. The random contact equation and its implications for (Colloidal) rods in packings, suspensions, and anisotropic powders. Langmuir 1996;12:1127e33.

[25] Shante VKS, Kirkpatrick S. An introduction to percolation theory. Adv Phys 1971;20:325-357.

[26] Isichenko, M. B. Rev. Mod. Phys. 1992, 64, 961.

[27] Boonstra, BB. Rubber Technology and Manufacture C.M. Blow and C. Hepburn (eds.), Newnes-Butterworths, London (1975).

[28] Flory PJ, Rehner, JJr. Statistical mechanics of cross-linked polymer networks II. Swelling. J Chem Phys 1943;11:521-526.

[29] Flory PJ, Rehner, JJr. Statistical theory of chain configuration and physical properties of high polymers. Ann N Y Acad Sci 1943;44:419 – 429.

[30] Leger, L, Creton, C. Adhesion mechanisms at soft polymer interfaces. Phil Trans R Soc A 2008;366:1425–1442.

[31] Raphael E, de Gennes, PG. Rubber-rubber adhesion with connector molecules. J Phys Chem 1992;96:4002-4007.